A Small Dual Purpose UHF RFID Antenna Design

A. Ali Babar[1], Leena Ukkonen[1], Atef Z. Elsherbeni[2], and Lauri Sydanheimo[1]

[1] Department of Electronics
Tampere University of Technology, Rauma Research Unit
Kalliokatu 2, FI-26100, Rauma, Finland
abdul.babar@tut.fi, leena.ukkonen@tut.fi, lauri.sydanheimo@tut.fi

[2] Department of Electrical Engineering
The University of Mississippi, University, MS 38677-1848, USA
atef@olemiss.edu

Abstract ─ In this paper, designs and development of a small dual purpose UHF RFID planar antenna and an RFID tag antenna for small wireless application devices are presented. The planar antenna resonates at both the European and US RFID bands. It has a reasonable gain on both RFID bands with an omni-directional radiation pattern. The RFID tag antenna is designed for the European UHF RFID band. Experimental results for radiation pattern, input impedance reflection coefficient, and tag antenna realized gain confirmed the validity of the designs based on numerical simulations.

Index Terms ─ Antenna, dual band antennas, microstrip, miniaturized, planar, reader antenna, RFID, tag antenna.

I. INTRODUCTION

The growing demand for small compact wireless devices has increased the need for small antennas that can be integrated while providing acceptable overall performance. Apart from the size of the antenna and the wireless device, the cost is one of the most important aspects to consider in developing a wireless system. Thus, small low-cost antenna models are needed. The European RFID band (865 MHz - 868 MHz) and the US RFID band (902 MHz - 928 MHz) can also be used for small wireless applications. This includes various wireless sensor networks and other small indoor consumer electronic systems.

Throughout the antenna design process in this paper, the main objective was to develop a low-cost small antenna model, with reasonable performance, for the UHF RFID European and US bands. This work is an extension to the previous antenna designed and presented in [1]. The current antenna design can be useful for developing reader antennas, as well as RFID tags [2-5]. Directionality of the antenna is a result of the patch part of the antenna which radiates more than the rest of the antenna components. Since the antenna operates for both European RFID and US RFID bands, it becomes a good candidate for use in low-cost global wireless devices. It is small in size and can be embedded and integrated in several small wireless units.

Similarly, the same antenna design can be utilized to operate as a tag antenna, with an omni-directional radiation pattern and reasonable gain. The tag antenna is designed by mirroring the top part of the planar antenna and eliminating the ground plane, leading to a symmetric dipole type structure. The tag antenna is designed to operate at the European UHF RFID band. The structure of the tag antenna makes it highly sensitive to any geometrical or dielectric change. This sensitivity behavior can be exploited to make the antenna work as a sensor tag. The antenna can also be tuned to work on other frequency bands, as well as multiple frequency bands, by changing some of its configuration parameters.

Planar antenna design techniques are discussed in Section II. Section III concentrates on

utilizing the same design to make a UHF RFID tag antenna. This is followed by the simulation and measurement process and results of the planar antenna and the RFID tag antenna in Section IV. Section V discusses the sensitivity of the RFID tag antenna relative to its geometrical parameters. This is followed by the conclusions in Section VI.

II. ANTENNA DESIGN

The antenna is designed and simulated with the help of Ansoft HFSS V. 12 [6]. A 1.6 mm thick FR-4 double-sided substrate with a relative dielectric constant of 4.1 is used. The outer dimension of the antenna is 42 mm in height and 30 mm in width. The patch or lower part of the antenna has copper on both sides of the substrate, whereas the upper part of the antenna has no copper under the substrate. The feed of the antenna (using SMA connector) is connected between the feeding block of width *'a'* and height *'b'* and the ground plane as shown in Fig. 2.

The antenna structure is fabricated on a low-cost FR4 substrate to provide a low-cost solution. Various miniaturization techniques were used to tune the microstrip antenna design to the desired frequency [7]. Extra lumped components, such as capacitors and inductors were avoided in order to reduce the anticipated gain and efficiency losses from these elements. This also simplifies the manufacturing process and reduces the cost of the antenna production.

The antenna design uses the miniaturization technique of shorting the antenna structure with the ground plane, similar to PIFA designs presented in [8-9]. The shorted antenna models have a great dependency on the ground plane, which itself works as part of an asymmetrical dipole structure.

Therefore, designing a small shorted antenna model, with a small ground plane, makes the ground plane a more effective radiator. This fact is exploited in the design to achieve an antenna that radiates more on one of its poles towards the negative 'y' axis. The upper part of the antenna, along the positive 'y' axis, which consists of microstrip lines, helps in matching the antenna to the desired operating frequencies [10]. For example, line '*k*', is divided into two microstrip lines *'m1'* and '*m2*', enabling the antenna to resonate at two different frequency bands.

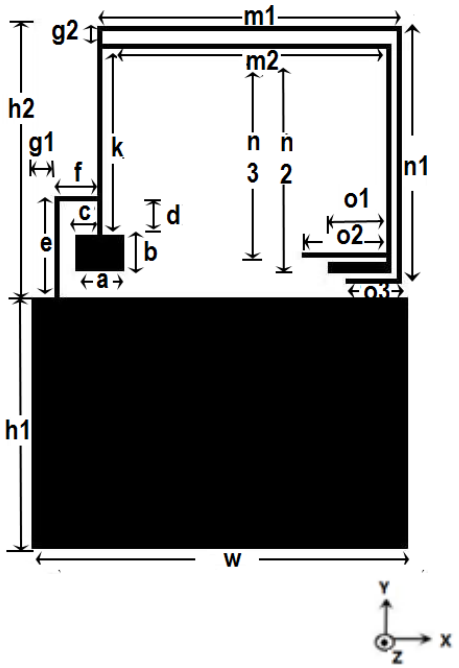

Fig. 1. Antenna configuration.

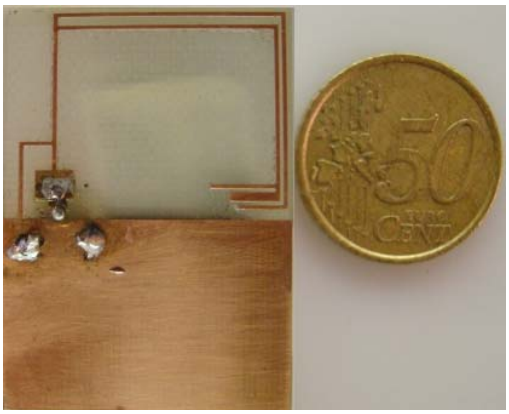

Fig. 2. Fabricated antenna model.

Furthermore, line '*m2*' is divided into two lines, '*o1*' and '*o2*'. The distance between the lines, at various places, plays a major role in matching the antenna. This also helps in lowering the resonance frequency of the antenna, by utilizing the current-vector alignment technique [11]. According to this, closely coupled lines with a current vector in-phase and in the same direction, increase the self-inductance of the antenna. This eventually reduces the resonance frequency of the antenna.

Table 1: The geometrical dimensions of the antenna in Fig. 1

Line (mm)	Length (mm)	Width (mm)
a	4	
b	3	
c	1.75	
d	2.5	0.5
e	8	0.5
f	3.45	0.5
g1	2	
g2	0.9	0.5
h1	20	
h2	21.5	
k	14.6	0.5
m1	24.25	0.5
m2	22.45	0.5
n1	20.5	0.5
n2	18.3	0.5
n3	17	0.5
o1	5.5	1
o2	6.7	0.5
o3	5	0.5
w	30	

III. TAG ANTENNA DESIGN

The RFID tag antenna is an extension of the small antenna design presented above [12]. The tag is designed using a 3.175mm thick Rogers RT/duroid 5880 [13] with a relative dielectric constant of 2.2 and 35µm copper cladding. Higgs 3 IC, manufactured by Alien Technology [14], is used in this tag antenna design. The antenna's configuration parameters were determined using numerical simulation based on Ansoft HFSS V.12. The size of the antenna is 44mm (height) x 30mm (width). The design of the tag antenna is similar to the planar small antenna, presented in Fig. 1 with slight changes in the structure. The changes are required to tune the tag antenna to the desired European UHF RFID frequency band (865 MHz - 868 MHz).

Figure 3, shows the design of the tag antenna, achieved by mirroring the planar antenna in Fig. 1. This makes the tag antenna a quasi symmetric dipole structure. There is no copper under the substrate, to achieve an omni-directional radiation pattern. The IC of the tag antenna lies in the middle of the two '*a*' lines. Line '*g*' connects both arms of the dipole to enhance the input inductance of the antenna. Some parameters of the planar antenna are modified to match the tag antenna to the desired frequency band and the input impedance of the IC. The resonance frequency of the tag antenna can be tuned to the desired frequency by changing the length of the tuning lines '*o*' and '*i*'. The length of line '*g*' also plays a great role in changing the resonance of the antenna and improving the antenna's return loss. Similar to the antenna design shown in Fig. 1, the coupling between the parallel lines reduces the size of the antenna. The closely coupled parallel lines increase the self inductance of the antenna, when the current vector is in-phase and in the same direction. The tag antenna design can also be tuned to operate on multiple frequency bands. This tuning can be done by varying the lengths of '*l*' and '*o*'. The dimensions of the tag geometrical parameters are listed in Table 2.

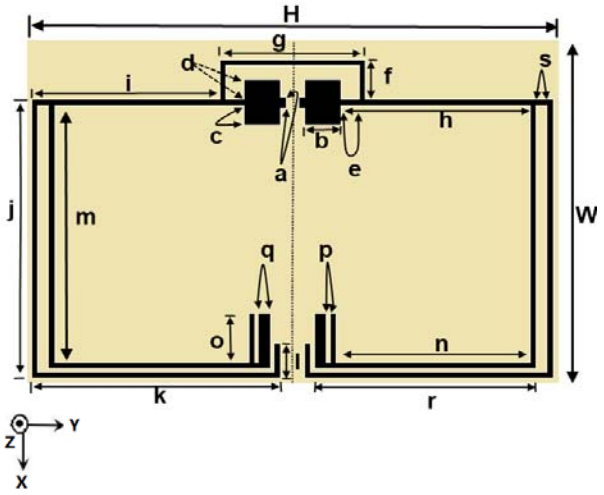

Fig. 3. UHF RFID tag antenna design.

The transfer of power between the IC (complex load impedance) and the tag antenna (complex source impedance), can be analyzed based on equation (1). The ratio of power available from the tag antenna (P_{tag}) and the power reflected back (P_{rfl}) is called the power reflection coefficient [15], [16].

$$\frac{P_{rfl}}{P_{tag}} = \left| \frac{Z_{ic} - Z_a^*}{Z_{ic} + Z_a} \right|^2 . \qquad (1)$$

Table 2: The geometrical dimensions of the antenna in Fig. 3

Line (mm)	Length (mm)	Width (mm)
a	0.5	1
b	3	
c	1.75	
d	1.75	
e	1.5	0.5
f	3.45	0.5
g	12	0.5
h	15.6	0.5
i	15.5	0.5
j	24.3	0.5
k	20.5	0.5
l	3	0.5
m	22.45	0.5
n	16	0.5
o	3.3	0.5
p	0.3	
q	1	
r	18.3	0.5
s	0.9	0.5
H	44	
W	30	

In equation (1), $Z_a=R_a+jX_a$ is the impedance of the tag antenna, whereas $Z_{ic}=R_{ic}+jX_{ic}$ is the impedance of the tag chip. The superscript (*) denotes the complex conjugate. For optimal power transfer and maximum read range, it is desirable to have a lower value for the power reflection coefficient at the operating frequency band.

IV. RESULTS

A. Planar antenna design

The antenna is fabricated with the help of a milling machine, and the S_{11} is measured by an Agilent 8358 (VNA series) Network Analyzer [17]. The radiation pattern and gain of the antenna are measured by Satimo's StarLab [18]. In Fig. 4, the simulated and measured S_{11} of the antenna are shown with resonances at both the European and the US RFID bands.

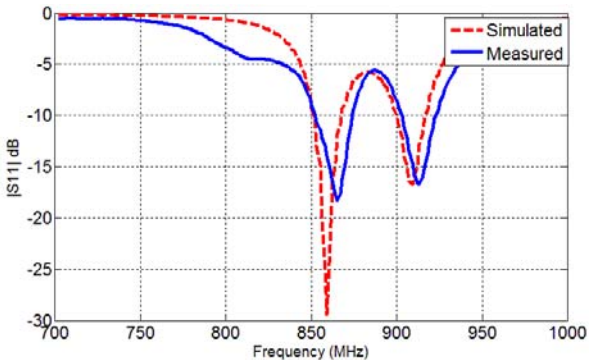

Fig. 4. Simulated and measured S_{11} (dB) of the planar antenna.

Figures 5 and 6 show the radiation patterns of the H (x-z) and E (x-y) planes of the antenna, respectively, for both 865MHz and 915MHz operating frequencies. No significant variations can be considered between the patterns at these two frequencies. Furthermore, one can observe that the directional characteristics of the antenna pattern lies in the half space below the x-z plane. The maximum deviation from the omni-directional characteristics in the H-plane is about 4dB. For the E-plane patterns, the side lobe level is in the order of -8dB, and the back lobe level is about -10dB, and -14dB for 865MHz and 915MHz, respectively. Figures 7 and 8 show the measured 3-D gain radiation patterns of the planar antenna at 865MHz and 915MHz, respectively. Similar patterns are observed, but with higher gain value at the higher frequency.

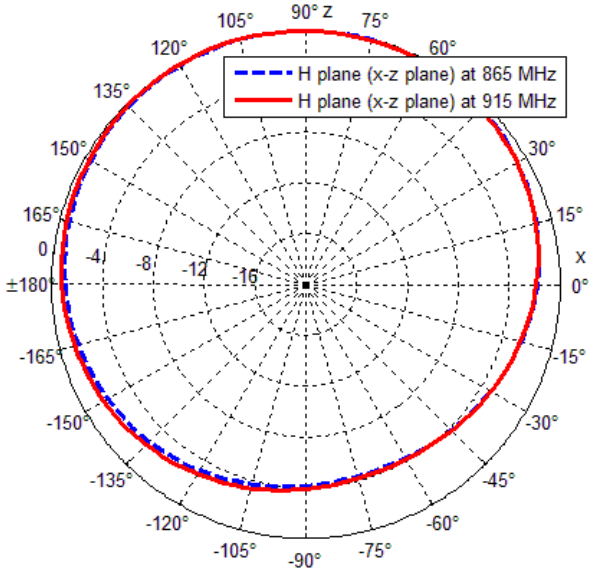

Fig. 5. Measured H-plane normalized gain (dB) of the planar antenna at 865 and 915MHz.

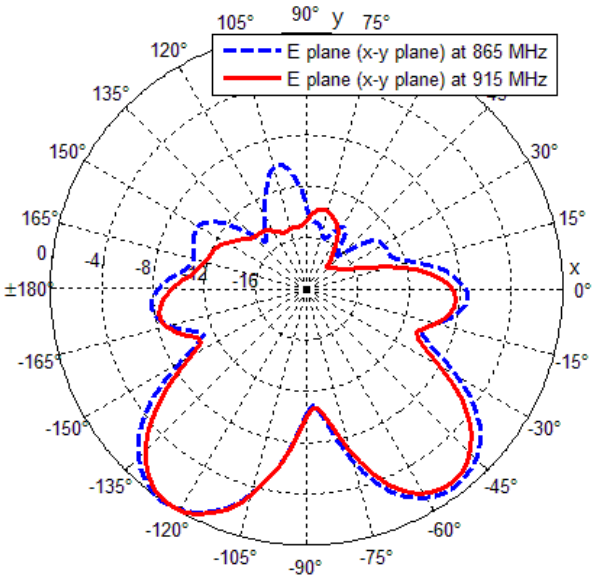

Fig. 6. Measured E-plane normalized gain (dB) of the planar antenna at 865 and 915MHz.

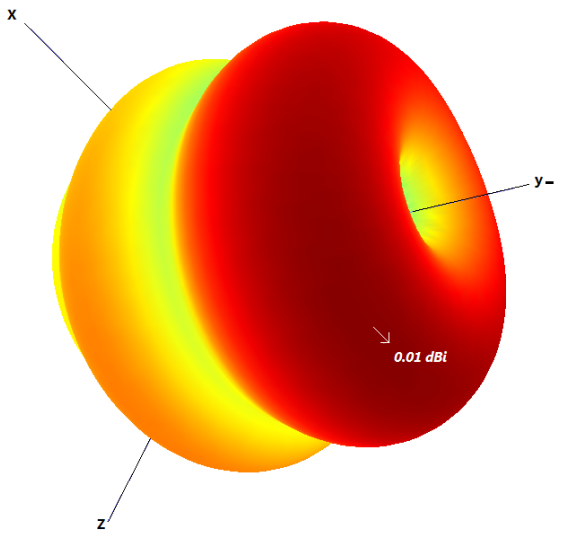

Fig. 7. Measured 3-D gain (dBi) radiation pattern of the planar antenna at 865MHz.

B. Tag antenna design

Figure 9 shows the power reflection coefficient of the tag antenna, resonating at the European UHF RFID band (865 MHz – 868 MHz). The centre frequency is set to 866 MHz. The figure illustrates that the tag antenna has a narrow bandwidth. This feature can be useful in applications where sensitive RFID tags are required. These applications include some of the RFID sensor applications, such as temperature and humidity sensors [19]. The input impedance of the chip and the tag antenna are shown in Fig. 10.

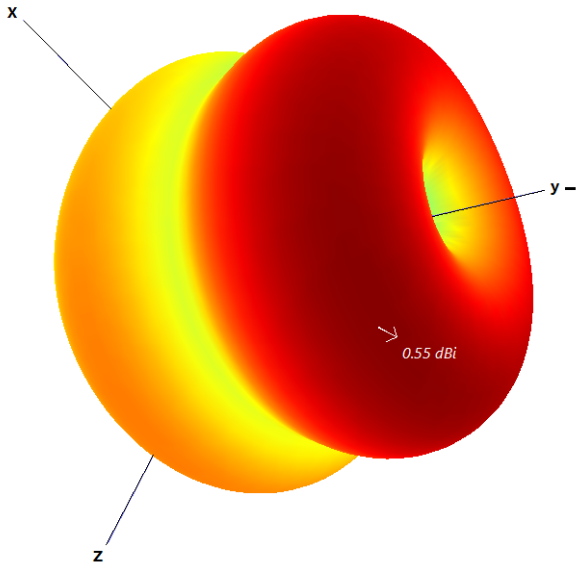

Fig. 8. Measured 3-D gain (dBi) radiation pattern of the planar antenna at 915MHz.

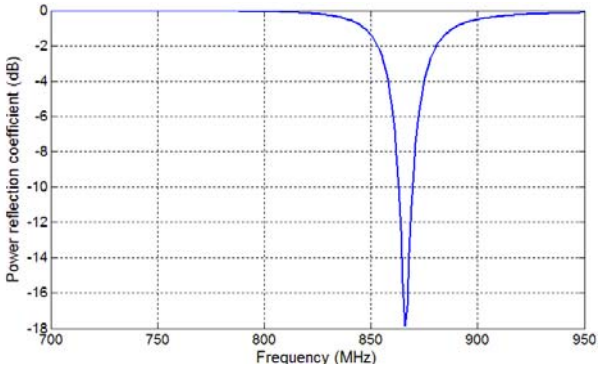

Fig. 9. Simulated power reflection coefficient of the tag antenna.

Figure 10 shows how the tag antenna parameters are carefully designed to provide a good conjugate match with the chip impedance. This is required to minimize the reflection loss at this junction, and hence improve the power transmission and maximize the read range.

The simulated normalized radiation patterns of the tag antenna are shown in Figs. 11 and 12 for the E and H planes, respectively. The radiation patterns show that the tag antenna has the typical radiation pattern of a dipole antenna.

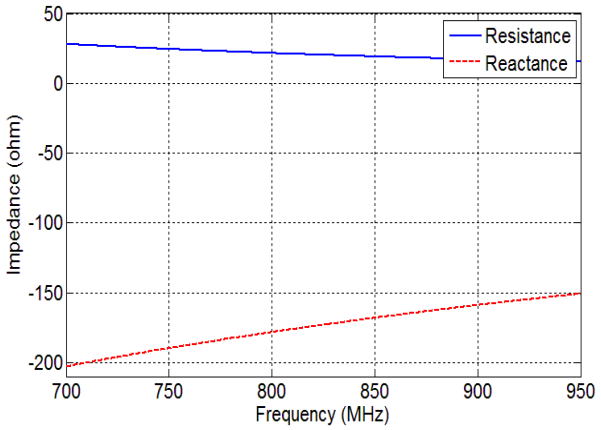

(a)

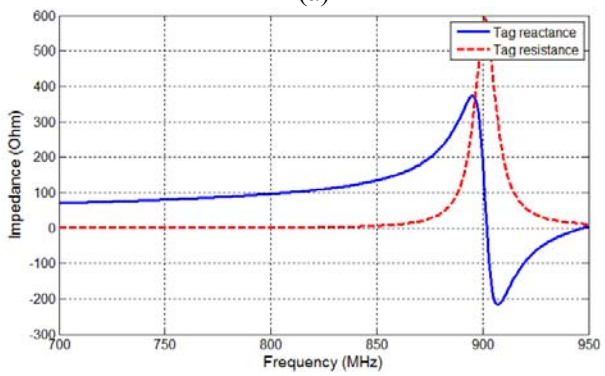

(b)

Fig. 10. Impedance versus frequency (a) chip impedance, (b) tag impedance.

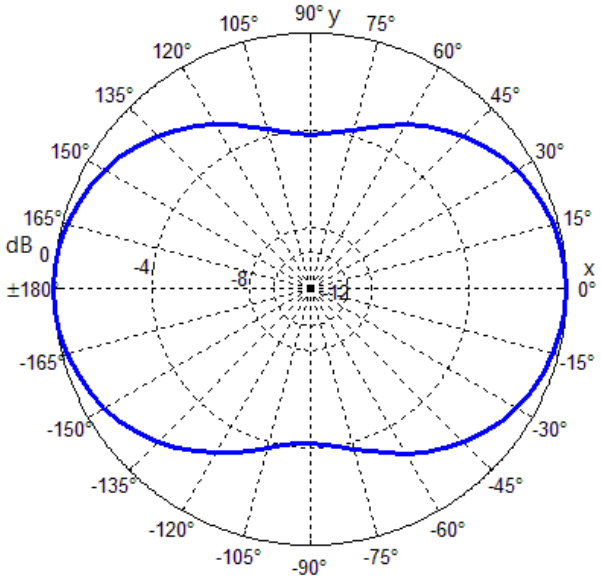

Fig. 11. Simulated E-plane (xy-plane) normalized gain (dB) of the radiation pattern of the tag antenna at 866MHz.

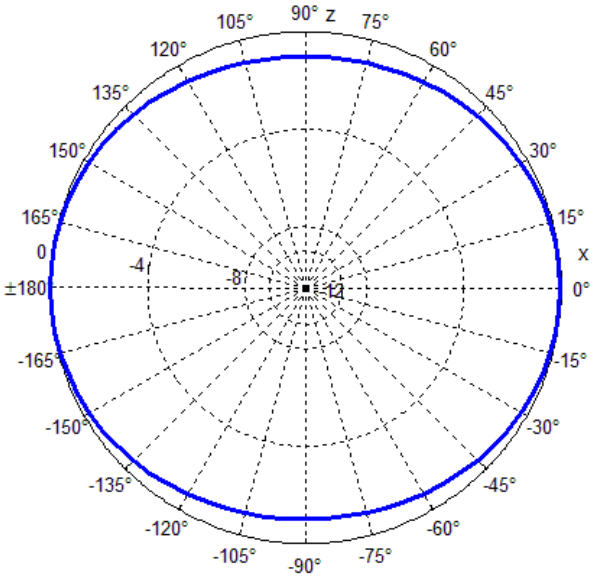

Fig. 12. Simulated H-plane (xz-plane) normalized gain (dB) of the radiation pattern of the tag antenna at 866MHz.

In Fig. 13, a 3-D view of the simulated radiation pattern of the tag antenna is shown, at 866MHz. As shown in the figure, the maximum simulated realized gain of the tag antenna at 866 MHz is approximately 1.4dBi, with asymmetric doughnut shape. The radiation pattern is not perfectly round, radiating slightly more along the x axis than that along the z axis.

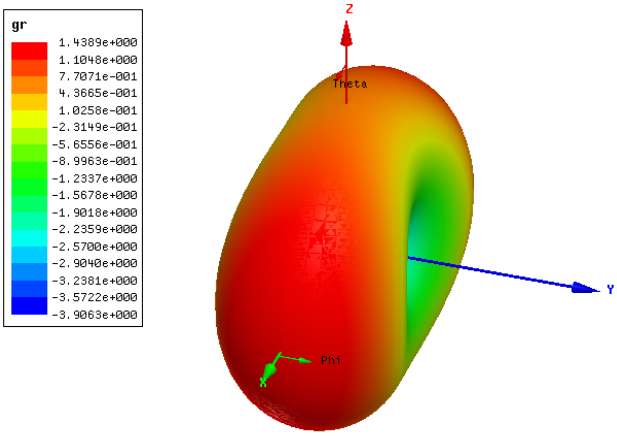

Fig. 13. 3-D view of the simulated realized gain (dBi) at 866MHz.

The fabricated model of the UHF RFID tag antenna model is shown in Fig. 14. This prototype was fabricated on Rogers 5880 substrate, with a

dielectric constant of 2.2. There is no copper on the opposite side of the substrate. This enables the tag antenna to achieve an almost omni-directional radiation pattern as shown in Fig. 13.

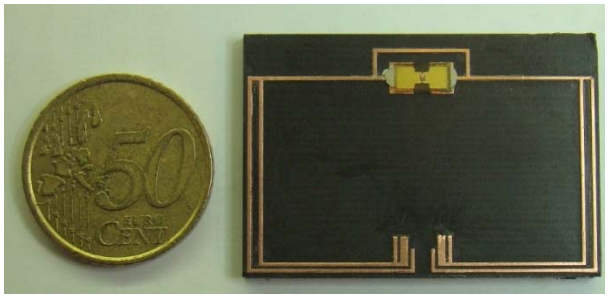

Fig. 14. Fabricated UHF RFID tag antenna.

A Tagformance RFID measurement device was used to measure the tag antenna in a specialized anechoic chamber suited for UHF RFID tag antennas [20]. The chamber contains a linearly polarized reader antenna, with a rotating disc to measure the radiation pattern of the tag. A linearly polarized reader antenna is connected to the Tagformance measurement device by Voyantic.

The theoretical read range of the tag antenna was calculated by using the measured results from the Tagformance, with the help of the following equation [23]:

$$d_{tag} = \frac{\lambda}{4\pi}\sqrt{\frac{1.64P_{ERP}}{L_{fwd}P_{th}}}. \qquad (2)$$

In the above equation, 'd_{tag}' is the theoretical read range of the tag antenna. 'L_{fwd}' is the measured path loss from the generator's output port to the input port of a hypothetic isotropic antenna placed at that tag's location. The forward path loss was achieved from the measured calibration data using the Tagformance measurement. The European effective radiated power 'P_{ERP}' value was considered equal to 2W (33dBm) according to [21]. The parameter 'P_{th}' is the measured threshold power in the forward direction from the transmitter to the tag. This is the minimum continuous wave power transmitted to enable the tag to send a response to EPC Gen 2 protocol's query command. The resulting theoretical read range of the tag antenna, calculated based on measured results, is shown in Fig. 15.

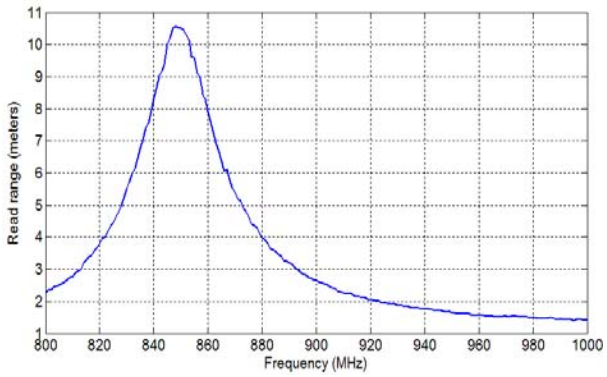

Fig. 15. Theoretical read range [d_{tag}] of the tag antenna.

In Fig. 15, the maximum read range is approximately 10.5m and is slightly shifted from 866MHz to 850MHz. This tag antenna is meant to be highly sensitive to structural changes. This nature of the tag antenna can be responsible for the shift of the frequency. The structural change can reasonably be caused by the inaccuracy of the fabrication process. Several other factors might also be responsible for the frequency shift including the process of attaching the IC strap to the tag antenna. This can be tuned by reducing the size of the two lines with length '*o*', by 1 - 2mm.

The maximum measured realized gain of the tag antenna can be analyzed by utilizing the path loss measurement data from the Tagformance measuring equipment. This can be described as [23],

$$G_r = \frac{P_{ic}}{L_{fwd} \cdot P_{th}}, \qquad (3)$$

where 'P_{ic}' is the sensitivity of the IC, which is equal to -18dBm, 'L_{fwd}' is the forward path loss from the transmitter to the tag antenna, and 'P_{th}' represents the threshold power. The estimated maximum simulated and measured gain of the tag antenna can be seen in Fig. 16. The difference between the simulated and measured realized gain can be due to several reasons. This includes the difficulty of simulating the actual substrate losses, and the inaccuracy of fabricating the tag. However, it is obvious that the maximum

measured gain is almost the same as the simulated gain at the desired operating frequency, 850MHz.

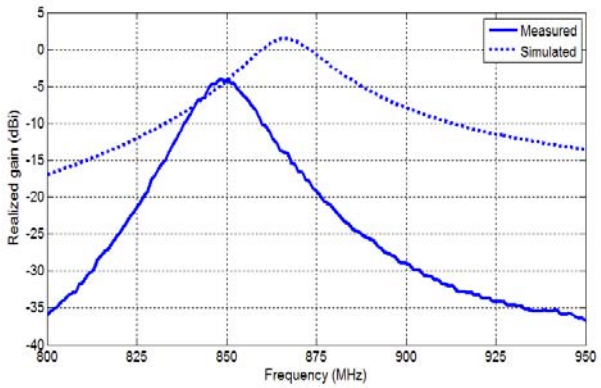

Fig. 16. Measured and simulated maximum realized gain of the tag antenna.

The measured normalized gain patterns at the E and H planes of the tag antenna are shown in Figs. 17 and 18, respectively. These measured radiation patterns resemble the simulated radiation patterns in Figs. 11 and 12, respectively, although at a slightly different frequency.

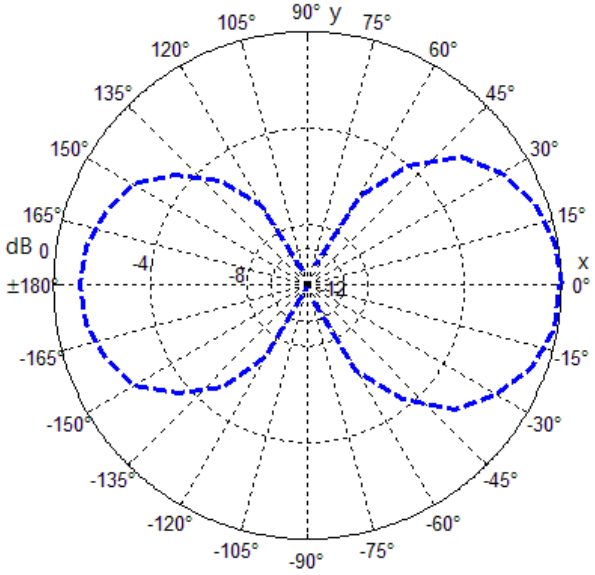

Fig. 17. Measured E-plane (xy-plane) normalized gain (dB) radiation pattern of the tag antenna at 850MHz.

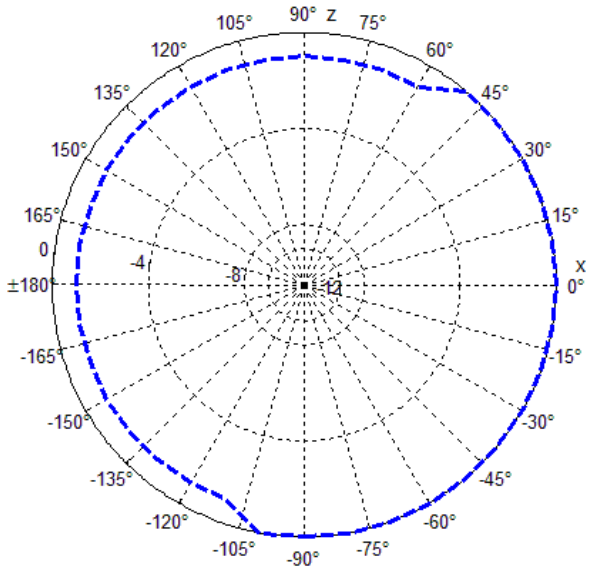

Fig. 18. Measured H-plane (xz-plane) normalized gain (dB) radiation pattern of the tag at 850MHz.

The measured normalized gain radiation pattern shown in Figs. 17 and 18, show an almost omni-directional radiation pattern as required for this application.

V. TAG SENSITIVITY ANALYSIS

Several parameters are useful for tuning the antenna to the desired frequency. Some of these are the substrate thickness, the shorting line '*g*', and the tuning lines '*l*' and '*o*'.

In Fig. 19, the resonance shift of the tag antenna, due to different substrate thicknesses is shown. According to the figure, reduction in the substrate thickness increases the resonance frequency of the tag antenna and vice versa. The rate of change of the resonance frequency is higher, with a decrease in the substrate thickness.

The length of the shorting line '*g*' can also be very useful in tuning the antenna. In Fig. 20, the effect of various lengths of the shorting line on the resonance frequency of the tag antenna is shown. According to the figure, a slight change in the length of the shorting line '*g*', directly influences the inductance and thus affects the resonance of the tag antenna.

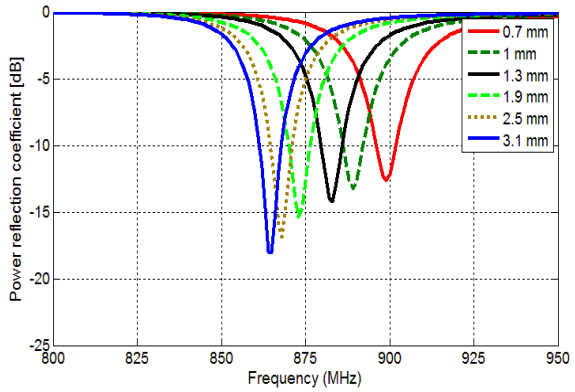

Fig. 19. Simulated power reflection coefficient of the tag antenna, due to various substrate thicknesses.

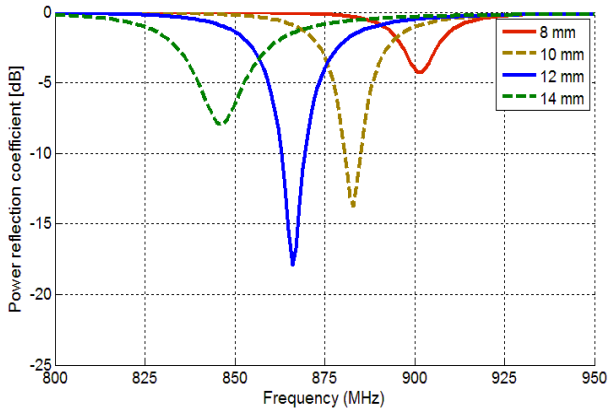

Fig. 20. Simulated power reflection coefficient of the tag antenna, due to various lengths of shorting lines '*g*'.

The tuning lines of length '*l*' and '*o*', can greatly help in fine tuning of the tag antenna. In Fig. 21, there is a gradual decrease in the resonance frequency, with an increase in the length of the tuning line '*l*'.

Similarly, the length '*o*' of the lines, can also be useful in tuning the tag antenna operating frequency. This effect is shown in Fig. 22, where the resonance frequency gradually changes with the increase in the length '*o*'. The lengths of the two lines equal to '*o*' are always kept same. The gap '*p*' between the two lines is also kept constant.

The above numerical results based on parametric study show that an antenna with small thin lines and small spacing between the lines helps miniaturize the antenna structure. However, such tag antennas exhibit narrowband characteristics and become sensitive to structural changes. These types of tag antennas can be useful for various sensing applications [22].

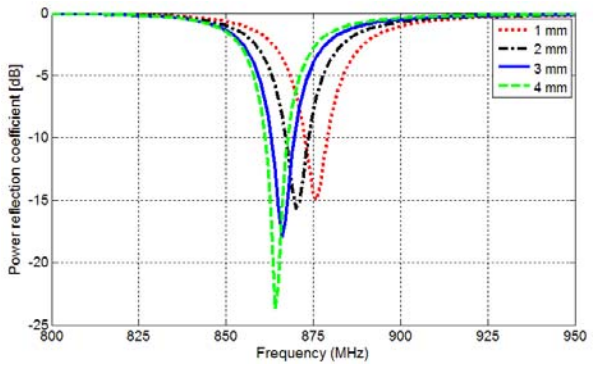

Fig. 21. Simulated power reflection coefficient shift of the tag antenna, due to various lengths of tuning line '*l*'.

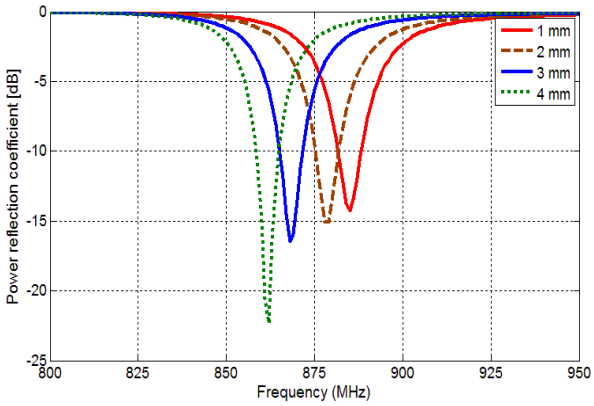

Fig. 22. Simulated power reflection coefficient of the tag antenna, due to various lengths of line '*o*'.

VI. CONCLUSION

In this paper, a small dual purpose planar RFID antenna design was discussed. The same antenna design is used as a shorted planar antenna, and as an RFID tag antenna. The planar shorted antenna works on both European and US RFID bands. Different miniaturization techniques helped in reducing the resonance frequency of the antennas. In the planar antenna model, the shorting technique and the close coupled lines helped in reducing the size of the antenna. The RFID tag antenna design's self inductance was increased with the help of the shorting line (loop) and the closely coupled lines, using current vector alignment technique. This indicates that the antenna structure can be reduced with the help of thin closely coupled lines. However, it makes the antenna more narrowband and sensitive. The

sensitivity of the antenna to the structural deformations can be utilized for various sensing tag antenna applications.

ACKNOWLEDGMENT

This research work has been funded by the Finnish Funding Agency for Technology and Innovation (TEKES), the Academy of Finland and the Centennial Foundation for Finnish Technology Industries, Finnish Cultural Foundation, Nokia Foundation and High Technology Foundation of Satakunta, Finland. The authors would also like to thank Toni Björninen for his assistance in conducting the measurements of the UHF RFID tag antenna.

REFERENCES

[1] A. A. Babar, L. Ukkonen, A. Z. Elsherbeni, and L. Sydanheimo, "Miniaturized Dual Band Planar Antenna," *26th Annual Review of Progress in Applied Computational Electromagnetics*, April, 2010.

[2] J. Landt, "The history of RFID," *IEEE Potentials*, vol. 24, no. 4, pp. 8-11, Oct. - Nov. 2005.

[3] K. Finkenzeller, *RFID Handbook, Radio-Frequency Identifications Fundamentals and Applications*, 2nd Ed. New York: Wiley, 2003.

[4] J.-P. Curty, N. Joehl, C. Dehollain, and M. J. Declercq, "Remotely powered addressable UHF RFID integrated system," *Solid-State Circuits, IEEE Journal*, vol. 40, no. 11, pp. 2193- 2202, Nov. 2005.

[5] W. C. Brown, "The history of power transmission by radio waves," *IEEE Trans. Microwave Theory Tech.*, vol. MTT-32, no. 9, pp. 1230-1242, Sept., 1984.

[6] ANSYS, Ansoft HFSS, http://www.ansoft.com/products/hf/hfss/

[7] P. Bhartia, I. Bahl, R. Garg, and A. Ittipiboon, *Microstrip Antenna Design Handbook*, *Artech House*, Inc. 2001.

[8] A. K. Skrivervik, J. –F. Zurcher, O. Staub, and J. R. Mosig, "PCS Antenna Design: The Challenge of Miniaturization," *IEEE Antennas and Propagation Magazine*, vol. 43, no. 4 August 2001.

[9] T. Taga and K. Tsunekawa, "Performance analysis of a built-in planar inverted-F antenna for 800MHz hand portable hand units," IEEE J. Select. Areas Commun., vol. 5, pp. 921-929, June 1987.

[10] K. –L. Wong, *Planar Antennas for Wireless Communications*, Wiley series in Microwave and Optical Engineering, 2003.

[11] S. R. Best and J. D. Morrow, "On the Significance of Current Vector Alignment in Establishing the Resonant Frequency of Small Space-Filling Wire Antennas," IEEE Antennas and Wireless Propagation Letters, vol. 2, 2003.

[12] D. M. Dopkins, The RF in RFID: Passive UHF RFID in Practice, Newline, 2008.

[13] Rogers corporation, Rogers RT/duroid 5880 high frequency laminates datasheet, http://www.rogerscorp.com/documents/606/acm/RT-duroid-5870-5880-Data-Sheet.aspx

[14] Alien technologies, Higgs 3 datasheet.

[15] http://www.alientechnology.com/docs/products/DS_H3.pdf

[16] K. Kurokawa, "Power Waves and the Scattering Matrix," Microwave Theory and Techniques, IEEE Transactions on, vol. 13, no. 2, pp. 194-202, Mar. 1965.

[17] P. V. Nikitin, K. V. S. Rao, S. F. Lam, V. Pillai, R. Martinez, and H. Heinrich, "Power reflection coefficient analysis for complex impedances in RFID tag design," Microwave Theory and Techniques, IEEE Transactions, vol. 53, no. 9, pp. 2721- 2725, Sept. 2005.

[18] Agilent Technologies, http://www.agilent.com

[19] Satimo Starlab, http://www.satimo.com

[20] J. Virtanen, L. Ukkonen, T. Björninen, and L. Sydänheimo, "Printed humidity sensor for UHF RFID systems," IEEE Sensors Applications Symposium (SAS), pp. 269-272, 23-25 Feb. 2010, Limerick, Ireland.

[21] Voyantic, RFID measurements solutions, http://www.voyantic.com

[22] EPC frequency regulations UHF, http://www.epcglobalinc.org/tech/freq_reg/RFID_at_UHF_Regulations_20100824.pdf

[23] A. Rida, L. Yang, and M. Tentzeris, RFID-Enabled Sensor Design and Applications, Artech House, Inc. 2010.

[24] J. Virtanen, T. Björninen, L. Ukkonen, and L. Sydänheimo, "Passive UHF Inkjet Printed Narrow Line RFID Tags," IEEE Antennas and Wireless Propagation Letters, vol. 9, pp. 440-443, May 2010.

Abdul Ali Babar received his M.Sc. in Radio Frequency Electronics (Electrical Engineering), from Tampere University of Technology in 2009 and works as a Research Scientist in RFID research group, Tampere University of Technology. He is currently working on his Ph.D. degree in the Department of Electronics in Tampere University of Technology. His area of research includes RFID systems, RFID reader and Tag antennas, miniaturized antenna and other Radio Frequency systems and their integration in wireless systems.

Leena Ukkonen received the M.Sc. and Ph.D. degrees in Electrical Engineering from Tampere University of Technology (TUT) in 2003 and 2006, respectively. She is currently leading the RFID research group at TUT Department of Electronics, Rauma Research Unit. She, also, holds Adjunct Professorship in Aalto University School of Science and Technology. She has authored over 90 scientific publications in the fields of RFID antenna design and industrial RFID applications. Her research interests are focused on RFID antenna development for tags, readers, and RFID sensors.

Lauri Sydänheimo received the M.Sc. and Ph.D. degrees in Electrical Engineering from Tampere University of Technology (TUT). He is currently a Professor with the Department of Electronics, TUT, and works as the Research Director of Tampere University of Technology's Rauma Research Unit. He has authored over 120 publications in the field of RFID tag and reader antenna design and RFID system performance improvement.
His research interests are focused on wireless data communication and radio frequency identification (RFID), especially RFID antennas and sensors.

Dr. Atef Z. Elsherbeni is a Professor of Electrical Engineering and Associate Dean of Engineering for Research and Graduate Programs, the Director of The School of Engineering CAD Lab, and the Associate Director of The Center for Applied Electromagnetic Systems Research (CAESR) at The University of Mississippi. In 2004, he was appointed as an adjunct Professor, at The Department of Electrical Engineering and Computer Science of the L.C. Smith College of Engineering and Computer Science at Syracuse University. In 2009, he was selected as Finland Distinguished Professor by the Academy of Finland and Tekes.

Dr. Elsherbeni is the co-author of the book "*The Finite Difference Time Domain Method for Electromagnetics With MATLAB Simulations*", SciTech 2009, the book "*Antenna Design and Visualization Using Matlab*", SciTech, 2006, the book "*MATLAB Simulations for Radar Systems Design*", CRC Press, 2003, the book *"Electromagnetic ScatteringUsing the Iterative Multiregion Technique"*, Morgan & Claypool, 2007, the book *"Electromagnetics and Antenna Optimization using Taguchi's Method"*, Morgan & Claypool, 2007, and the main author of the chapters "*Handheld Antennas"* and "*The Finite Difference Time Domain Technique for Microstrip Antennas"* in Handbook of Antennas in Wireless Communications, CRC Press, 2001.

Dr. Elsherbeni is a Fellow member of the Institute of Electrical and Electronics Engineers (IEEE) and a Fellow member of The Applied Computational Electromagnetic Society (ACES). He is the Editor-in-Chief for ACES Journal and an Associate Editor to the Radio Science Journal.